

# Incomplete Descriptor Mining with Elastic Loss for Person Re-Identification

Hongchen Tan, Xiuping Liu\*, Yuhao Bian, Huasheng Wang, and Baocai Yin

**Abstract**—In this paper, we propose a novel person Re-ID model, Consecutive Batch DropBlock Network (CBDB-Net), to capture the attentive and robust person descriptor for the person Re-ID task. The CBDB-Net contains two novel designs: the Consecutive Batch DropBlock Module (CBDBM) and the Elastic Loss (EL). In the Consecutive Batch DropBlock Module (CBDBM), we firstly conduct uniform partition on the feature maps. And then, we independently and continuously drop each patch from top to bottom on the feature maps, which can output multiple incomplete feature maps. In the training stage, these multiple incomplete features can better encourage the Re-ID model to capture the robust person descriptor for the Re-ID task. In the Elastic Loss (EL), we design a novel weight control item to help the Re-ID model adaptively balance hard sample pairs and easy sample pairs in the whole training process. Through an extensive set of ablation studies, we verify that the Consecutive Batch DropBlock Module (CBDBM) and the Elastic Loss (EL) each contribute to the performance boosts of CBDB-Net. We demonstrate that our CBDB-Net can achieve the competitive performance on the three standard person Re-ID datasets (the Market-1501, the DukeMTMC-Re-ID, and the CUHK03 dataset), three occluded Person Re-ID datasets (the Occluded DukeMTMC, the Partial-REID, and the Partial iLIDS dataset), and a general image retrieval dataset (In-Shop Clothes Retrieval dataset).

**Index Terms**—Person Re-ID, Dropout strategy, Triple Ranking, Incomplete Person Descriptor

## I. INTRODUCTION

Person Re-Identification (Re-ID) has attracted increasing attention from both the academia and the industry due to its significant role in the video surveillance. Given a target person image captured by one camera, the goal of the person Re-ID task is to re-identify the same person from images captured by other cameras' viewpoints. Despite the exciting progress in recent years, the person Re-ID task remains to be extremely

(Corresponding author: Xiuping Liu)

Hongchen Tan, Xiuping Liu, Yuhao Bian, and Huasheng Wang are with School of Mathematical Sciences, Key Laboratory of Computational Mathematics, Dalian University of Technology, Dalian 116024, China (e-mail: tanhongchen-phd@mail.dlut.edu.cn/tanhongchenphd@126.com; xpliu@dlut.edu.cn; yhbian@mail.dlut.edu.cn; huashengdadi@mail.dlut.edu.cn).

Baocai Yin is with the Department of Electronic Information and Electrical Engineering, Dalian University of Technology, Dalian 116024, China (e-mail: ybc@dlut.edu.cn).

Copyright©2021 IEEE. Personal use of this material is permitted. However, permission to use this material for any other purposes must be obtained from the IEEE by sending an email to [pubs-permissions@ieee.org](mailto:pubs-permissions@ieee.org).

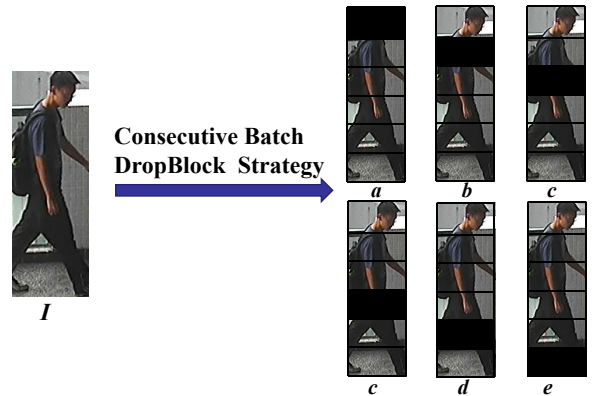


Fig. 1. To easily understand the Consecutive Batch DropBlock (CBDB) strategy, we directly use the raw person image to show the operation of our CBDB strategy. In fact, the Consecutive Batch DropBlock (CBDB) strategy is conducted on the conv-layer.

challenging. This is because the task is easily affected by body misalignment, occlusion, background perturbation, and viewpoint changes, etc. To tackle this challenge, almost person Re-ID approaches focus on two strategies: feature descriptor learning and distance metric learning. The former approaches aim to capture the discriminative person descriptor which is robust to various interference factors; The latter approaches aim to gain a better metric space equipped with better classification discrimination of different persons.

Recently, many outstanding approaches [85], [16], [25], [42], [63], [36], [77], [55], [2], [48], [78], [83], equipped with a series of metric constraints, try to capture the global descriptor of the whole person image. However, the global descriptors are easily prone to the false matching between persons who look similar, due to lacking enough local information. Therefore, other approaches [5], [27], [7], [40], [51], [64], [66] introduce the pose estimation or human parsing models to help the person Re-ID model better locate and capture local human part feature. However, the underlying datasets bias between pose estimation, human parsing, and person Re-ID remains an obstacle against the ideal human body partition on person images. And the additional human models make the person Re-ID model more complex and unwieldy. Thus, in this paper, we aim to design a simple and effective strategy to help the person Re-ID model capture a high-quality person descriptor.

Recently, the Dropout strategies [54], [50], [17], [85], [80], [10], is widely used in person Re-ID and other visual tasks. Compared with the additional human model assistance, these

Dropout strategies are the lightweight and effective for person Re-ID models. It can better help the person Re-ID model embed in the application device. In these Dropout strategies, Cutout [10], random erasing [80], and SpatialDropout [54], can randomly drop the feature pixel in the feature maps or feature vectors. However, these methods only belong to a regularization method and not attentive feature learning methods. And they can not drop a large contiguous area within a training batch. So, Batch DropBlock [85] is proposed to drop the same continuity region in a training batch. Inspired by the Batch DropBlock strategy in [85], our first idea is to propose a novel drop strategy, Consecutive Batch DropBlock (CBDB), to produce multiple incomplete feature maps for capturing high-quality person descriptor.

Different from Batch DropBlock: **(i)** our Consecutive Batch DropBlock strategy can gain multiple incomplete feature maps to train the deep Re-ID model; **(ii)** our consecutive Batch DropBlock drops the same patch for the whole training set instead of a batch. As shown in the Figure 1, for the Consecutive Batch DropBlock, we firstly conduct uniform partition on the conv-layer. Secondly, we independently and continuously drop each patch from top to bottom on the conv-layer. Since this, we can gain multiple incomplete feature maps to push the deep model to capture the robust and high-quality person feature descriptor. Thus, our Consecutive Batch DropBlock is an effective attentive feature learning strategy. Besides, the Consecutive Batch DropBlock strategy can be regarded as the Batch DropBlock' [85] extension, and the complementary strategy to uniform patch descriptors in PCB [53]. Thus, we believe that the Consecutive Batch DropBlock (CBDB) strategy can effectively improve the robustness of person descriptors in the person Re-ID task.

Based on the Consecutive Batch DropBlock, we can gain multiple incomplete feature maps (descriptors) in the training process. However, inevitably there will be hard sample pairs and easy sample pairs for the person matching task. The Batch Hard Triplet Loss [23] may be a suitable metric loss function to balance these hard sample pairs. However, in the whole training process, the difficulty level of hard sample pairs are different in different training stage; In the whole training sets, the difficulty level of hard sample pairs are also different in different person ID. So, our second idea is to design a novel metric loss function to dynamically balance the hard sample pairs and easy sample pairs in the training process.

Based on the above analysis, we propose a novel person Re-ID model, Consecutive Batch DropBlock Network (CBDB-Net). The CBDB-Net contains two novel designs: the Consecutive Batch DropBlock strategy and the Elastic Loss. The former exploits multiple incomplete descriptors to improve the robustness of the deep model. And, in the testing stage, a simple test model is adopted to produce a high-quality person descriptor for the person matching. The latter can better mine and balance the hard sample pairs for the whole training samples in the whole training process. It can further improve the performance of the deep person Re-ID model.

In the experimental section, firstly we validate our CBDB-Net on three generic person Re-ID datasets: Market-1501 [76], DukeMTMC-reID [41], [75], CUHK03 [31]. Secondly, we

evaluate our CBDB-Net on three occluded person Re-ID datasets: Occluded-DukeMTMC [38], Partial-REID [60], and Partial-iLIDS [21]. Finally, we believe our CBDB-Net can be applied to other image retrieval tasks. So, we evaluate our CBDB-Net on the In-Shop Clothes retrieval dataset [37]. Extensive experimental results and analysis demonstrate the effectiveness of CBDB-Net and significantly improved performance compared against most state of the arts over two evaluation metrics.

## II. RELATED WORK

### A. Part-based person Re-ID Models

In our CBDB-Net, the Consecutive Batch DropBlock strategy can guide the person Re-ID model to gain multiple incomplete feature maps of one person image in the training process. These incomplete feature maps can be regarded as the large parts. So, in this subsection, we introduce related works of the part-based person Re-ID task. Recently, [27], [46], [63], [51], [72] adopted an additional human body part detector or an additional human body parsing model to focus on more accurate human parts. E.g., SPReID [27] applied an additional human body parsing model to generate 5 different pre-defined body part masks to capture more reliable part representations. [19] addressed the missed contextual information by exploiting both the accurate human body parts and the coarse non-human parts. [38], [57] combined the pose landmarks and uniform partial feature to improve the performance of the occluded person Re-ID task. [59] adopted the key point detector to exploit three coarse body part, and combine the global information to conduct the person matching. Different from [59], [68] dropped the keypoint detector, only used the maximum feature responses to locate the body regions and combined with the Part Loss. [53] conducted uniform partition on the conv-layer for learning part-level features. Our CBDB-Net also belongs to part-based person Re-ID methods to some degree. Similar to [53], [68], we also needn't any additional human models' assistance. In the CBDB-Net, we can gain multiple large parts by the proposed Consecutive Batch DropBlock strategy. These large feature parts can be regarded as complementary to the uniform parts in [53], [68]. And, compared with the small feature parts in [59], [53], [68], these large feature parts can better encourage the deep Re-ID model to capture the robust person structural information.

### B. Triplet Ranking in person Re-ID

Triplet Ranking Loss [47] is one of the most important metric loss functions, which encourages the distance between positive sample pairs to be closer than negative sample pairs. It has been applied in various outstanding deep vision models, and achieves outstanding performance in these metric learning tasks. [49] may be the first one to introduce the Triplet Loss into the Re-ID task. When SPGAN [9] conducted the cross-domain person Re-ID task, they adopted the Contrastive Loss to preserve the person ID information in the cross-domain image style transfer. [2] extended the Triplet Loss by introducing the absolute distance of the positive sample pair. [44] proposed a virtual sample in the triplet unit to

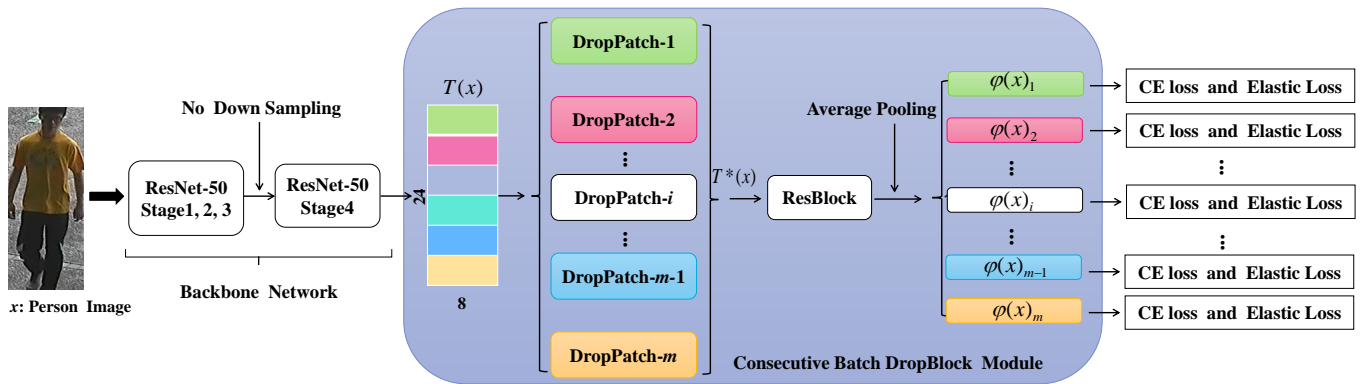


Fig. 2. The architecture of Consecutive Batch DropBlock Network (CBDB-Net) for the person Re-ID task. The two novel strategies are Consecutive Batch DropBlock Module and the proposed Elastic Loss. Here the “CE” denotes the Cross-Entropy Loss function.

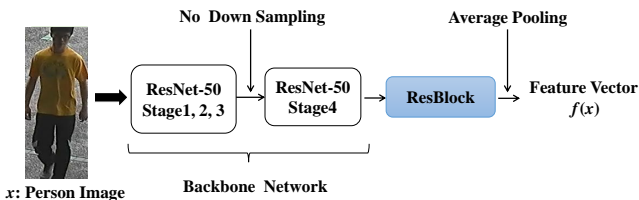


Fig. 3. The network pipeline of the proposed CBDB-Net in the testing stage.

accelerate sample distance optimization. Similar to [11], [23] proposed the batch hard Triplet Loss by introducing the hard sample mining strategy for person sample pairs. Since this, many SOTA Re-ID methods [26], [1], [62], [61], [43], [85] adopted the Batch Hard Triplet Loss to gain the outstanding performance.

Inspired by these methods [26], [1], [62], [61], [43], [85], we also introduce the hard sample mining strategy to design a novel triplet loss in our CBDB-Net. Different from the original Batch Hard Triplet Loss [23], our proposed triplet loss can dynamically adjust the learning weights of hard sample pairs in the whole training process. The experiments show that it can further help the person Re-ID model to gain better performance.

### III. CBDB-NET

In this section, we describe the details of the proposed Consecutive Batch DropBlock Network (CBDB-Net). The training framework is shown in Figure 2; The testing framework is shown in Figure 3.

**In the training stage.** As shown in Figure 2, our CBDB-Net contains three components: the Backbone Network, the Consecutive Batch DropBlock Module (CBDBM), and the loss functions (which contain our proposed Elastic Loss). The input to the Backbone Network is the person image  $x$ . The Backbone Network provides the basic feature maps  $T(x)$  for the Consecutive Batch DropBlock Module (CBDBM). The core of the Consecutive Batch DropBlock Module (CBDBM) is the Consecutive Batch DropBlock strategy. The input of the CBDBM is the basic feature maps  $T(x)$ . The CBDBM outputs

multiple incomplete person descriptors  $\varphi(x)_i, i = 1, 2, \dots, m$ . The loss functions constraint the whole CBDB-Net to capture the robust and high-quality person information for the person matching task. The loss functions contain the Cross-Entropy Loss and our proposed Elastic Loss.

**In the testing stage.** As shown in Figure 3, the testing framework contains the Backbone Network, ResBlock, and Average Pooling Operation. We use the feature  $f(x) \in \mathbb{R}^{512}$  to find the best matching person in the gallery by comparing the squared distance, i.e.  $d(a, b) = \|a - b\|_2^2$ .

In the following parts, we mainly describe the training framework of our CBDB-Net. We describe the details of Backbone Network in Subsection III-A, the details of Consecutive Batch DropBlock Module (CBDBM) in Subsection III-B, the details of the proposed Elastic Loss in Subsection III-C, and the Network Architecture Overview III-D.

#### A. Backbone Network

Following current many outstanding methods [26], [1], [62], [61], [43], [85], our CBDB-Net also uses the ResNet-50 [20] pre-trained on ImageNet [8] as the backbone network, to encode a person image  $x$ . To get a larger size high-level feature tensor, we also modify the basic structure of the ResNet-50 slightly. The down-sampling operation at the beginning of the “ResNet-50 Stage 4” is not employed. Therefore, we can get a larger feature tensor  $T(x) \in \mathbb{R}^{24 \times 8 \times 2048}$ .

#### B. Consecutive Batch DropBlock Module

Based on the large feature tensor  $T(x) \in \mathbb{R}^{24 \times 8 \times 2048}$ , we build the Consecutive Batch DropBlock Module (CBDBM).

(i:) As shown in Figure 2, the tensor  $T(x)$  is divided to  $m$  uniform patches. (ii:) The *DropPatch* -  $i, i = 1, 2, \dots, m$  is designed to drop the  $i$ -th patch on the tensor  $T(x)$ . As shown in the Figure 4, the feature tensor  $T(x)$  is divided to 6 uniform patches; The *DropPatch* - 3 is used to drop the 3-th patch on the tensor  $T(x)$ . We can see that the 3-th patch on the  $T(x)$  is zeroed out. Since this, we can gain  $m$  incomplete feature tensors  $T(x)_i^* \in \mathbb{R}^{24 \times 8 \times 2048}, i = 1, 2, \dots, m$ . (iii:)

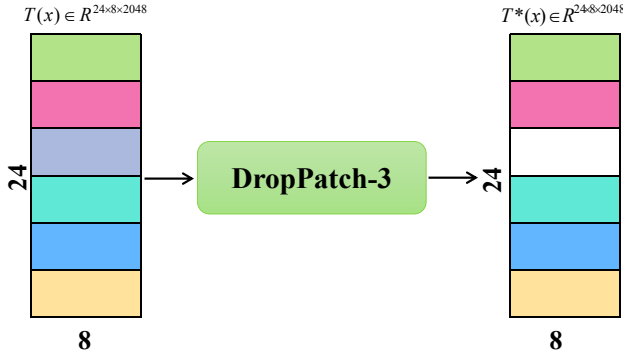


Fig. 4. An example of *DropPatch-3*'s operation. The *DropPatch-3* is used to drop the 3-th patch on the tensor  $T(x)$ . So, we can see that the 3-th patch on the  $T(x)$  are zeroed out.

These  $m$  incomplete feature tensors  $T(x)_i^* \in \mathbb{R}^{24 \times 8 \times 2048}$ ,  $i = 1, 2, \dots, m$  are fed into the “ResBlock” and average pooling operation. Since this, we can gain  $m$  incomplete person descriptors, i.e.  $\varphi(x)_i \in \mathbb{R}^{512}$ ,  $i = 1, 2, \dots, m$  which is fed into the loss functions: the Cross-Entropy Loss and the proposed Elastic Loss III-C. Here, the “ResBlock” is composed of three bottleneck blocks [20].

**Analysis.** Based on the person feature map  $T(x)$ , one patch feature region on the  $T(x)_i^*$  is missed. In the training stage, the person Re-ID loss functions can push the model to capture key person information for Re-ID from the remaining areas on the  $T(x)_i^*$ . Our CBDBM can produce multiple incomplete feature maps  $T(x)_i^*$ ,  $i = 1, 2, \dots, m$ . Since this, the deep Re-ID model is required to adapt to different patch dropout cases to capture key person information. In the testing stage, as shown in Figure 3, the CBDBM is moved. Thus, the deep Re-ID model can better extract robust and key person information from the whole person image feature.

### C. The proposed Elastic Loss

The CBDBM outputs  $m$  incomplete descriptors  $\varphi(x)_i \in \mathbb{R}^{512}$ ,  $i = 1, 2, \dots, m$  of one person image  $x$ . In the training process, these incomplete descriptors inevitably contain many hard matching sample pairs. Recently, the Batch Hard Triple (BHT) Loss [23] introduced the hard sample mining strategy to effectively focus on the hard sample pairs in the training process. However, the hard sample mining strategy in the Batch Hard Triple Loss [23] did not consider the two issues: **(a)** in the different training stage, the difficulty level of hard samples pairs are different; **(b)** in each training step or epoch, the difficulty level of hard samples pairs from variant ID person are also different. Recently, Focal Loss [35] introduced the weight control item into the Cross-Entropy Loss, which can dynamically adjust the weight of hard samples and easy samples in the training process. Inspired by the Focal Loss [35] and the Batch Hard Triple Loss [23], we propose a novel Elastic Loss to relieve the above two issues.

To define the Elastic Loss, we **firstly** organize the training samples into a set of triplet feature units,  $S =$

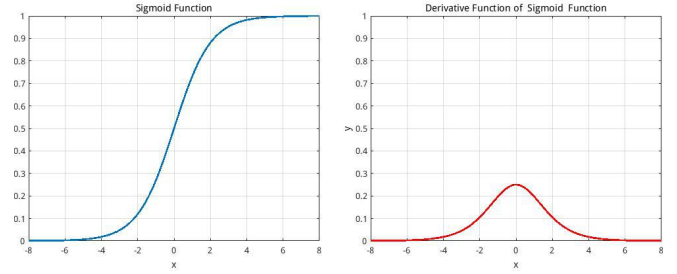


Fig. 5. The function curve and derivative function curve of the sigmoid function. As  $x$  gets bigger, the value of the sigmoid function gets closer and closer to 1. As  $x$  gets gets closer and closer to 0, the value of the sigmoid function gets closer and closer to  $\frac{1}{2}$ . It can effectively control the weight of the Batch Hard Triplet Loss in  $[\frac{1}{2}, 1)$ .

$(s(x^a), s(x^p), s(x^n))$  which simply denotes as  $S = (s^a, s^p, s^n)$ , and the raw person image triplet units is  $X = (x^a, x^p, x^n)$ . Here,  $(s^a, s^p)$  represents a positive pair's feature with  $y^a = y^p$ , and  $(s^a, s^n)$  indicates a negative pair's feature with  $y^a \neq y^n$ . Here,  $y \in Y$  is the person ID information. We use  $d(a, b) = \|a - b\|_2^2$  to denote the squared distance between the feature vectors  $a$  and  $b$  in the feature space.

**Secondly**, we revisit the Batch Hard Triplet Loss [23]. Based on the Triplet Loss [47], [23] extended the Triplet Loss [47] by introducing the hard sample mining strategy. Here, the hard sample mining strategy in the training batch: the positive sample pair with the largest distance as the hard positive sample pair; the negative sample pair with the smallest distance as the hard negative sample pair. In the training process, the hard sample pair will be focused on. Based on the design, the Batch Hard Triple Loss function is defined as:

$$\mathcal{T}_{HardTriplet} = [\eta + \max_{x^a, x^p} d(s^a, s^p) - \min_{x^a, x^n} d(s^a, s^n)]_+ \quad (1)$$

Here,  $\eta$  represents the margin parameter.

**Finally**, we define the Elastic Loss by revising the Batch Hard Triplet Loss. Same as the Eq. 1, the hard positive sample pairs is the maximum distance between  $s^a$  and  $s^p$ , i.e.  $\max_{x^a, x^p} d(s^a, s^p)$ , within the training batch; and the hard negative sample pairs is the minimum distance between  $s^a$  and  $s^n$ , i.e.  $\min_{x^a, x^n} d(s^a, s^n)$ , within the training batch. To dynamically adjust sample pairs' weights, we design a novel weight control item. **(i)** We introduce the “nuclear weight term”,  $\delta = \frac{\max_{x^a, x^p} d(s^a, s^p)}{\min_{x^a, x^n} d(s^a, s^n) + \varepsilon}$  ( $\varepsilon = 10^{-6}$ ). The parameter

$\varepsilon$  is to prevent the denominator from being 0. The “nuclear weight term” can adaptively adjust the weights of loss function under the hard positive sample pairs and the hard negative sample pairs. When the distance of hard positive sample pairs becomes larger or the distance of hard negative sample pairs becomes smaller, the  $\delta$  becomes larger. It indicates that the loss function pays more attention to the current person ID's hard sample pairs in the current training step, and vice versa.

In the ideal training goal, the  $\max_{x^a, x^p} d(s^a, s^p)$  is smaller than the  $\min_{x^a, x^n} d(s^a, s^n)$ . However, in fact, we observe that

the  $\max_{x^a, x^p} d(s^a, s^p)$  is usually larger than the  $\min_{x^a, x^n} d(s^a, s^n)$  for many person ID sample pairs. If we directly use the  $\delta$  to adjust the weight of the Batch Hard Triplet Loss, the  $\delta$  brings too much weight fluctuation, which is not conducive to model training. Therefore, we hope the weights of  $\delta$  can fluctuate over a small range. (ii:) Based on the  $\delta$ , we design a ‘‘Shell function’’, i.e.  $g(x) = \frac{1}{1 + e^{-x}}$ , which is the sigmoid function. It can effectively control the  $\delta$  in  $[\frac{1}{2}, 1)$ . In this way, the weight will not fluctuate too much. And, the easy sample pairs can also get appropriate weights to participate in the effective training of the person Re-ID model.

For the sigmoid function, we can see the function curve and the derivative function curve in Figure 5. As  $x$ , i.e.  $\delta$  in our weight control item, gets bigger, the value of the sigmoid function gets closer and closer to 1. And the value of the derivative function is smaller. It indicates that the weight of the difficult sample is stable at around 1. In the process of the parameter optimization process, the gradient of the Batch Hard Triplet Loss can gain a large learning weight. As  $x$ , i.e.  $\delta$  in our weight control item, gets closer and closer to 0, the value of the sigmoid function gets closer and closer to  $\frac{1}{2}$ . When  $\delta$  is around 0, the value of the derivative function is large. So, for the easy sample pairs, the loss function gives a flexible and small weight to focus on them.

Based on the ‘‘nuclear weight term’’ and ‘‘Shell function’’, our final weight control item is  $\frac{1}{1 + e^{-\delta}}, \delta = \frac{\max_{x^a, x^p} d(s^a, s^p)}{\min_{x^a, x^n} d(s^a, s^n) + \varepsilon}$ . We introduce the weight control item into the Batch Hard Triplet Loss to help the Re-ID model better focus on hard sample pairs. Besides, as described in [23], in person Re-ID task, it can be beneficial to pull together samples from the same class as much as possible [3], [71]. Inspired by [23], we use the softplus function  $\ln(1 + e^x)$ , the Batch Hard Triplet Loss [23], and our proposed weight control item to build our Elastic Loss, i.e.

$$\mathcal{L}_{Elastic} = \ln(1 + \exp(\frac{1}{1 + e^{-\delta}} (\max_{x^a, x^p} d(s^a, s^p) - \min_{x^a, x^n} d(s^a, s^n)))) \quad (2)$$

Where  $\delta = \frac{\max_{x^a, x^p} d(s^a, s^p)}{\min_{x^a, x^n} d(s^a, s^n) + \varepsilon}$  and  $\varepsilon = 10^{-6}$ . Now, we extend our Elastic Loss to the whole triplet units in our CBDB-Net, which can be formulated as follows:

$$\mathcal{L}_{Elastic}(X) = \frac{1}{|X|} \sum_{(x^a, x^p, x^n) \in X} \sum_{i=1}^m \mathcal{T}_{Elastic}(\varphi(x^a)_i, \varphi(x^p)_i, \varphi(x^n)_i) \quad (3)$$

where  $|X|$  indicates the number of triplet units in each training batch.

#### D. Network Architecture Overview

In this subsection, we revisit the network architecture and summary loss functions of our CBDB-Net in the training stage.

The overall pipeline of our CBDB-Net is illustrated in Figure 2 in the training stage. The Backbone Network firstly takes a person image  $x$  as input, and then outputs the feature map  $T(x) \in \mathbb{R}^{24 \times 8 \times 2048}$ . Secondly, the feature  $T(x)$  is fed into Consecutive Batch DropBlock Module (CBDBM). The CBDBM can output multiple incomplete feature descriptors  $\varphi(x)_i \in \mathbb{R}^{512}, i = 1, 2, \dots, m$ . Finally, the Cross-Entropy loss and the Elastic Loss are also employed at last. The whole loss functions in training stage are listed as:

$$\mathcal{L}_{all}(X) = \mathcal{L}_{Elastic}(X) + \sum_{j=1}^M \sum_{i=1}^m \mathcal{L}_{CE}(\varphi(x)_{ij}) \quad (4)$$

Here,  $\varphi(x)_i \in \mathbb{R}^{512}, i = 1, 2, \dots, m$ ;  $\mathcal{L}_{CE}(\cdot)$  is the Cross-Entropy Loss for person ID classification. The batch size  $M$  in the training stage is 64.

## IV. EXPERIMENT

In this section, we evaluate the CBDB-Net qualitatively and quantitatively. To evaluate the effectiveness of our CBDB-Net, we conduct extensive experiments on three generic person datasets (the Market-1501 [76], the DukeMTMC-reID [41], [75], and the CUHK03 [31]), three occluded Person Re-ID datasets (the Occluded-DukeMTMC [38], the Partial-REID [60], and the Partial-iLIDS [21]) and one clothes image retrieval dataset (In-Shop Clothes Retrieval dataset [37]). Firstly, we discuss various ablation studies on the four datasets (the Market-1501 [76], the DukeMTMC-reID [41], [75], the CUHK03 [31], and the In-Shop Clothes Retrieval dataset [37]) to validate the effectiveness of each strategy in our CBDB-Net. Secondly, we compare the performance of CBDB-Net against many state-of-the-art methods on these seven datasets.

### A. Datasets and Evaluation

**Market-1501 [76]** contains 32, 668 labeled images of 1, 501 identities which is collected from 6 different camera views. Following almost person Re-ID approaches, the whole 1, 501 identities are split into two non-overlapping fixed person ID sets: the training set contains 12, 936 person images from 751 identities; the testing set contains 19, 732 person images from other 750 identities. In the testing stage, we use 3368 query images from 750 test person identities to retrieval the same ID persons from the rest of the test set, i.e. the gallery set.

**DukeMTMC-reID [41], [75]** is also a large-scale person Re-ID dataset. The DukeMTMC-reID contains 36, 411 labeled images of 1, 404 identities which is collected from 8 different camera views. The training set contains 16, 522 person images from 702 identities; In the testing stage, we use 2, 228 query images from the other 702 identities, and 17, 661 gallery images.

**CUHK03 [31]** is the most challenging of these three generic person Re-ID datasets. It composed of 14, 096 images of 1, 467 identities captured from 6 cameras. It provides bounding boxes detected from manual labeling and deformable part

models (DPMs), the latter type is more challenging due to severe bounding box misalignment and cluttered background. Following [84], [26], [85], [53], we use the 767/700 split [31] with the detected images.

**Occluded-DukeMTMC [38]** contains 15,618 training images, 17,661 gallery images, and 2,210 occluded query images. The Occluded-DukeMTMC is introduced by [38]. We use this dataset to demonstrate that our CBDB-Net also can achieve good performance on the occluded Person Re-ID task.

**Partial-REID [60]** is a specially designed partial person Re-ID dataset which contains 600 images from 60 person identities. And each person has 5 partial images in the query set and 5 full-body images in the gallery set. These images are collected at a university campus from different viewpoints, backgrounds, and different types of severe occlusion.

**Partial-iLIDS [21]** is a simulated partial person Re-ID dataset based on the iLIDS dataset. It has a total of 476 images of 119 person identities.

**In-shop clothes retrieval [37]** is a clothes image retrieval dataset. It contains 11,735 classes of clothing items with 54,642 images. The training set contains 25,882 images from 3,997 classes; the testing set contains 28,760 images from 3,985 classes. The test set is divided into the query set of 3,985 classes (14,218 images) and the gallery set of 3,985 classes (12,612 images). We apply our CBDB-Net on the clothes image retrieval task to evidence that our CBDB-Net can be suitable for other image retrieval tasks.

**Evaluation Protocol.** We employ two standard metrics as in most person Re-ID approaches, namely the mean Average Precision (mAP) and the cumulative matching curve (CMC) used for generating ranking accuracy. We use Rank-1 accuracy and mAP to evaluate the effectiveness of our CBDB-Net on all seven datasets.

*B. Implementation Details*

Following many outstanding approaches [61], [85], [58], [4], [38], [82], the input images are re-sized to  $384 \times 128$  and then augmented by random horizontal flip and normalization in the training stage. In the testing stage, the images are also re-sized to  $384 \times 128$  and augmented only by normalization. Based on the pre-trained ResNet-50 backbone, our network is end-to-end in the whole training stage. Our network is trained using 2 single GTX 2080Ti GPUs with a batch size of 64. Each batch contains 16 identities, with 4 samples per identity. We use the Adam optimizer [30] with 400 epochs. The base learning rate is initialized to  $1e-3$  with a linear warm-up [18] in the first 50 epochs, then decayed to  $1e-4$  after 200 epochs, and further decayed to  $1e-5$  after 300 epochs.

*C. Ablation Study of CBDB-Net*

*1) Discussion of the number of DropPatches  $m$ :*

In this subsection, we mainly discuss the influence of the number of DropPatches  $m$  on the performance of the CBDB-Net. In our CBDB-Net, the size of  $T(x)$  is  $24 \times 8 \times 2048$ . When  $m = 2, 3, 4, 6, 8, 12$ ,  $24\%m = 0$ . When  $m = 5, 7, 9, 10, 11$ ,  $24\%m \neq 0$ . In the Figure 6, there are two kind Consecutive Batch DropBlock strategies: in Figure 6 (a), there is no overlap

TABLE I  
RESULTS OF CBDB-NET ON THE CUHK03-DETECTED AND MARKET-1501 DATASETS UNDER DIFFERENT NUMBER OF BRANCHES IN THE PROPOSED CBDB-NET.

Method	CUHK03-Detected		Market-1501	
	Rank-1	mAP	Rank-1	mAP
m=2	58.4%	56.2%	89.0%	74.6%
m=3	74.2%	69.2%	93.6%	83.8%
m=4	75.7%	71.1%	94.0%	85.1%
m=5	75.9%	71.9%	94.1%	84.6%
m=6	76.6%	72.8%	94.4%	85.0%
m=7	76.3%	73.0%	94.3%	85.0%
m=8	76.2%	72.6%	94.3%	84.8%
m=9	76.4%	72.6%	94.4%	84.9%
m=10	76.5%	72.7%	94.3%	84.7%
m=11	74.6%	70.4%	93.9%	84.0%
m=12	75.9%	72.5%	94.3%	84.4%

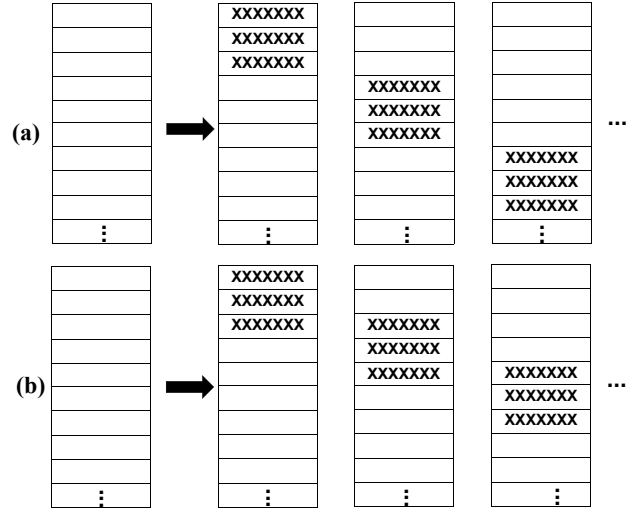


Fig. 6. Various versions of the Consecutive Batch DropBlock strategy. The figure (a) is the Consecutive Batch DropBlock strategy in Figure 4. There is no overlap areas between the dropped patch by  $DropPatch - (i)$  and dropped patch by  $DropPatch - (i + 1)$ . The figure (b) is the other Consecutive Batch DropBlock strategy. There is an overlap area between the dropped patch by  $DropPatch - (i)$  and dropped patch by  $DropPatch - (i + 1)$ .

between the dropped patch by  $DropPatch - (i)$  and dropped patch by  $DropPatch - (i + 1)$ ; in Figure 6 (b), there is an overlap area between the dropped patch by  $DropPatch - (i)$  and dropped patch by  $DropPatch - (i + 1)$ . When  $24\%m = 0$ , we adopt the dropout pattern of Figure 6 (a) to build our CBDB-Net. When  $24\%m \neq 0$ , we adopt the dropout pattern of Figure 6 (b) to build our CBDB-Net. As shown in Table I, we show the results of our CBDB-Net under the different value  $m$  in the CUHK03-Detected and Market-1501 datasets. When  $m$  is equal to 6, our CBDB-Net achieves the best performance on these two datasets. So, in our CBDB-Net, we set the number of DropPatches is 6, i.e.  $m = 6$ .

*2) Effectiveness of the each strategy in the CBDB-Net:*

In this subsection, we mainly discuss the effectiveness of each component in our CBDB-Net on four datasets: Market-1501, DukeMTMC-reID, CUHK03-Detected, and In-shop clothes retrieval datasets.

**(I.)** To demonstrate the effectiveness of the proposed Elastic Loss, we use the IDE+BHT[85], [77] as the baseline model.

TABLE II

RESULTS PRODUCED BY COMBINING DIFFERENT COMPONENTS OF THE CBDB-NET. THE PARAMETER  $m$  IN THIS TABLE IS 6. CBDB-NET<sup>†</sup>: WE DIRECTLY CONCATENATE THE  $\varphi(x)_i \in \mathbb{R}^{512}, i = 1, 2, \dots, 6$  TO CONDUCT THE PERSON MATCHING TASK IN THE TESTING STAGE. IDE+CBDB-NET CONTAINS  $m + 1$  BRANCHES:  $m$  INCOMPLETE FEATURE BRANCHES AND A GLOBAL BRANCH FROM IDE [85], [77]. THE TRAINING PIPELINE AND TESTING PIPELINE OF THE IDE+CBDB-NET ARE SHOWN IN FIGURE 8 AND FIGURE 9 RESPECTIVELY. CBDBM\* = CBDB-NET W/O THE ELASTIC LOSS = IDE+CBDBM W/O THE GLOBAL BRANCH FROM IDE [85], [77]. BHT IS SHORT FOR BATCH HARD TRIPLE LOSS. EL IS SHORT FOR ELASTIC LOSS. THE BOLD IS THE BEST RESULT.

Method	Market-1501		DukeMTMC-reID		CUHK03-Detected		CUHK03-Labeled		Clothes	
	Rank-1	mAP	Rank-1	mAP	Rank-1	mAP	Rank-1	mAP	Rank-1	mAP
IDE+BHT [85], [77]	93.1%	80.6%	84.4%	68.4%	63.6%	60.0%	67.4%	61.5%	89.9%	72.0%
IDE+EL	93.9%	82.5%	85.9%	71.2%	69.9%	65.9%	70.3%	66.5%	91.7%	73.8%
IDE+CBDBM	94.2%	84.4%	87.3%	73.6%	75.3%	71.8%	77.6%	74.7%	91.2%	73.6%
CBDBM*	94.0%	84.7%	86.5%	70.7%	74.7%	71.5%	75.7%	73.2%	91.0%	73.1%
CBDB-Net	<b>94.4%</b>	85.0%	87.7%	74.3%	<b>76.6%</b>	72.8%	<b>78.3%</b>	<b>75.9%</b>	92.0%	75.4%
CBDB-Net w/o "ResBlock"	93.8%	83.7%	86.5%	72.2%	73.4%	69.5%	76.6%	73.0%	91.8%	74.4%
CBDB-Net <sup>†</sup>	<b>94.4%</b>	<b>85.2%</b>	87.3%	73.9%	74.9%	72.0%	77.8%	75.5%	92.1%	75.6%
IDE+CBDB-Net	94.3%	85.0%	<b>88.0%</b>	<b>74.4%</b>	<b>76.6%</b>	<b>73.1%</b>	77.8%	75.4%	<b>92.2%</b>	<b>75.6%</b>

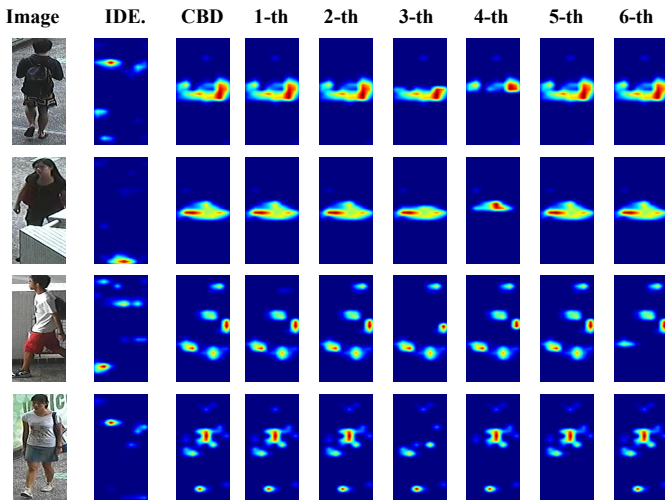


Fig. 7. Visualization of attention maps from Baseline, CBDB-Net and six branches ( $m=6$ ) of the CBDB-Net. The attention maps of Baseline are in the 1-st and 2-nd column; The attention maps of our CBDB-Net are in the 3-rd column; The attention maps of six branches ( $m=6$ ) of the CBDB-Net are from the 4-th column to the 9-th column respectively.

Here, BHT is short for Batch Hard Triple Loss. Based on the IDE+BHT, we replace Batch Hard Triplet Loss with the proposed Elastic Loss, i.e. "IDE+EL". Compared with IDE+BHT, our IDE+EL gains the obvious improvements on the four datasets over two measures. It effectively evidences the effectiveness of our Elastic Loss.

(II:) To demonstrate the effectiveness of the Consecutive Batch DropBlock Module (CBDBM), we also use the IDE+BHT[85], [77] as the baseline model. We demonstrate the validity of the CBDBM in two similar ways. (a:) We introduce the CBDBM into IDE+BHT[85], [77], i.e. IDE+CBDBM. Compared with IDE+BHT, our IDE+CBDBM also gains the obvious improvements in the four datasets over two measures. Besides, in the "IDE+CBDBM", the testing feature vector is composed of the feature vector  $f(x)$  (Dimension=512) and a global feature vector  $g(x)$  (Dimension=512) from the global branch in IDE [85], [77]. The testing pipeline of the "IDE+CBDBM" can be regarded as the pipeline shown in

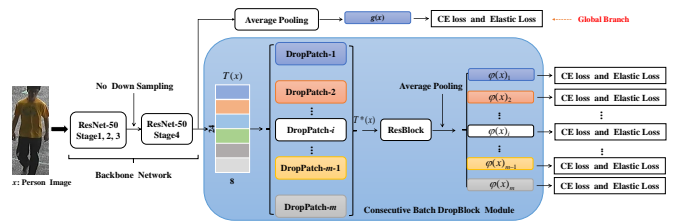


Fig. 8. The architecture of the IDE+CBDB-Net for the person Re-ID task. The IDE [85], [77] contains the Backbone Network, Average Pooling, CE Loss and Elastic Loss. The "CE" denotes the Cross-Entropy Loss function.

Figure 9. (b:) We drop out the global feature branch in the "IDE+CBDBM", i.e. "CBDBM\*". Here, CBDBM\* = CBDB-Net w/o the Elastic Loss = IDE+CBDBM w/o the global branch from IDE [85], [77]. As shown in Table II, compared with IDE+BHT, our CBDBM\* also gains the obvious improvements on the four datasets over two measures. Besides, from the 4-th column to the 9-th column in Figure 7, each branch in CBDBM can also capture the key information from the various incomplete feature maps.

(III:) Our CBDB-Net contains two novel designs: the Consecutive Batch DropBlock Module (CBDBM) and the Elastic Loss. As shown in Table II, compared with IDE+BHT[85], [77], our CBDB-Net achieves better performance. Besides, as shown in Figure 7, compared with Baseline (IDE+BHT [77]), our CBDB-Net can capture more key person information. **The CBDB-Net is our proposed novel person Re-ID model in this paper.** The CBDB-Net's training model is shown in Figure 2, and CBDB-Net's testing model is shown in Figure 3. In the testing stage, we use the 512 dimension feature vector  $f(x)$  to conduct the person matching task.

(IV:) In our CBDB-Net, based on the CBDBM, we can gain multiple incomplete feature maps. As shown in Figure 2, we append the additional "ResBlock" and average pooling operation on these incomplete feature tensors to gain incomplete person descriptors. To evidence the influence of the "ResBlock", we directly append the average pooling operation on these incomplete feature tensor  $T^*(x)$  to conduct the person retrieval task, i.e. CBDB-Net w/o "ResBlock". The results in Table II show that the "ResBlock" also plays an important role

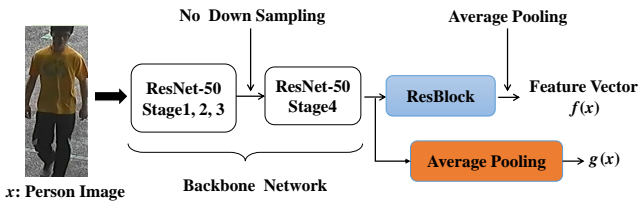


Fig. 9. The network pipeline of the IDE+CBDB-Net or IDE+CBDBM in the testing stage. The concatenation between vector  $f(x)$  and  $g(x)$  is the feature vector in the testing stage.

in the person matching task.

(V:) We further concatenate the  $\varphi(x)_i \in \mathbb{R}^{512}, i = 1, 2, \dots, 6$ , CBDB-Net<sup>†</sup>, and then use  $6 \times 512$  dimension feature vector to conduct the person matching. As shown in Table II, the CBDB-Net<sup>†</sup> can not achieve a better performance than that of the CBDB-Net. Even on the DukeMTMC, CUHK03-Detected, and CUHK03-Labeled datasets, the performance of the CBDB-Net<sup>†</sup> is worse than that of the CBDB-Net. And compared with CBDB-Net, the dimension of the feature vector of the CBDB-Net<sup>†</sup> in the testing stage is much higher than that of the CBDB-Net. It indicates that the feature  $f(x)$  of CBDB-Net is a high quality and robust global descriptor for the person matching task.

(VI:) Our CBDB-Net does not contain the global feature vector from the global branch of IDE [77]. So, we introduce the global branch into the CBDB-Net, i.e. IDE+CBDB-Net. The training pipeline and testing pipeline of the IDE+CBDB-Net are shown in Figure 8 and Figure 9 respectively. The concatenation between vector  $f(x)$  and  $g(x)$  is the feature vector in the testing stage. Compared with CBDB-Net, the IDE+CBDB-Net only gains a slight improvement. It indicates that the additional global branch does not make an effective contribution to the improvement of the person Re-ID task. To keep the model simple, we select the CBDB-Net as our proposed novel person Re-ID model in this paper.

### 3) Comparison with Various Dropout Strategies:

In this subsection, we discuss the performance of various Dropout strategies on the CUHK03-Detected dataset. (i:) Dropout [50] randomly drops the neural node of input feature maps or vector, which is regarded as a kind of regularization strategy to prevent overfitting of deep models. (ii:) Compared with Dropout, SpatialDropout [54] further randomly zeroes whole channels of the input feature tensors. And the channels of feature tensors to zero-out are randomized. (iii:) Based on the SpatialDropout, Batch Dropout randomly zeroes the whole channels of the input feature tensors within the whole batch. However, the Batch Drop can not drop a large contiguous area. (iv:) So, the DropBlock [17] strategy randomly drops a contiguous region on the feature maps. (v:) the Batch DropBlock further randomly drops the same region for every input tensor within a batch. Different from the Batch DropBlock [85], our Consecutive Batch DropBlock can drop the same region for every input tensor within the whole training set and product multiple incomplete feature tensors. As shown in Table III, compared with these Dropout strategies, our Consecutive Batch DropBlock strategy achieves the best performance on

TABLE III  
THE COMPARISON WITH A SERIES OF DROPOUT STRATEGIES ON THE CUHK03-DETECTED DATASET. THE BOLD IS THE BEST RESULT.

Method	CUHK03-Detected	
	Rank-1	mAP
SpatialDropout [54]	60.5%	56.8%
Dropout [50]	65.3%	62.2%
Batch Dropout [85]	65.8%	62.9%
DropBlock [17]	70.6%	67.7%
Batch DropBlock [85]	72.8%	69.3%
CBDB	<b>75.3%</b>	<b>71.8%</b>

the CUHK03-Detected dataset over two measures.

### 4) Discussion of the model size and testing time:

In this subsection, we mainly discuss the model size and testing time between our CBDB-Net and other SOTA person Re-ID models. As shown in Table IV, we list the Model Size, Testing Vector Dimension, and Testing Time of our CBDB-Net and other SOTA person Re-ID models on the Market-1501 test set.

(I) **Model Size.** The Backbone Network of these methods listed in Table IV is ResNet-50. The released code of these methods (include our CBDB-Net) is PyTorch. The model size listed in Table IV is the size of “.pth” document. Compared with BDB [85], PCB [53], PGFA [38], and ABD-Net [1], the model size of our CBDB-Net is the smallest.

(II) **Testing Vector Dimension.** As shown in Table IV, the testing vector of our CBDB-Net is only 512, which is much smaller than that of BDB [85], PCB [53], PGFA [38], and ABD-Net [1].

(III) **Testing Time.** As shown in Table IV, we list the testing time of these Re-ID models on the Market-1501 test set. We run the test experiments on an Intel Core i7 – 7820 CPU@3.60Hz  $\times$  16, with 64GB RAM and an RTX 2080 Ti GPU. As shown in Table IV, the testing time of our CBDB-Net is the shortest.

Above all, our CBDB-Net is a simple and effective person Re-ID model.

TABLE IV  
THE MODEL SIZE, TESTING VECTOR DIMENSION, AND THE TESTING TIME OF OUR CBDB-Net AND OTHER PERSON RE-ID MODELS ON THE MARKET-1501 DATASET.

Method	CBDB-Net	BDB [85]	PCB [53]	PGFA [38]	ABD-Net [1]
Model size	<b>100M</b>	129.4M	109.2M	110M	264M
Dimension	<b>512</b>	1536	12288	1792	2048
Testing Time	<b>37s</b>	42s	120s	172s	106s

### D. Comparison to State-of-the-art Methods

Firstly, we evaluate the performance of CBDB-Net on the generic person Re-ID task. We compared our CBDB-Net against the many state-of-the-art approaches on Market-1501, DukeMTMC-Re-ID and CUHK03, as shown in Tables V respectively. From the Table V, we can observe that our CBDB-Net achieves competitive performance on these three generic person Re-ID datasets and outperforming most published approaches by a clear margin. Specifically, CBDB-Net obtains 94.4% Rank-1 and 85.0% mAP, which outperforms

TABLE V

THE COMPARISON WITH MANY STATE-OF-THE-ART PERSON RE-ID APPROACHES ON THE MARKET-1501, THE DUKEMTMC-REID AND THE CUHK03 DATASETS. THE RESULTS OF THE "CBDB-NET+RE-RANKING" ARE BOLD. IN ADDITION TO THE "CBDB-NET+RE-RANKING", THE FIRST, SECOND AND THIRD HIGHEST SCORES ARE SHOWN IN RED, GREEN AND BLUE RESPECTIVELY. WE SET  $m = 6$ .

Method	Market-1501		DukeMTMC-reID		CUHK03-Detected		CUHK03-Labeled	
	Rank-1	mAP	Rank-1	mAP	Rank-1	mAP	Rank-1	mAP
MCAM[6]	83.8%	74.3%	-	-	46.7%	46.9%	50.1%	50.2%
MLFN [65]	90.0%	74.3%	81.0%	62.8%	52.8%	47.8%	54.7%	49.2%
SPReID[28]	92.5%	81.3%	84.4%	71.0%	-	-	-	-
HA-CNN [32]	91.2%	75.7%	80.5%	63.8%	41.7%	38.6%	44.4%	41.0%
PCB+RPP[53]	93.8%	81.6%	83.3%	69.2%	62.8%	56.7%	-	-
Mancs[56]	93.1%	82.3%	84.9%	71.8%	65.5%	60.5%	-	-
JSTL_DGD+ICV-ECCL [13]	88.4%	69.5%	-	-	-	-	-	-
PAN [74]	82.8%	63.4%	71.6%	51.5%	36.3%	34.0%	36.9%	35.0%
Camstyle[82]	88.1%	68.7%	75.3%	53.5%	-	-	-	-
FANN[45]	90.3%	76.1%	-	-	69.3%	67.2%	-	-
VCFL[12]	90.9%	86.7%	-	-	70.4%	70.4%	-	-
PGFA [38]	91.2%	76.8%	82.6%	65.5%	-	-	-	-
SVDNet+Era [84]	87.1%	71.3%	79.3%	62.4%	48.7%	37.2%	49.4%	45.0%
TriNet+Era[84]	83.9%	68.7%	73.0%	56.6%	55.5%	50.7%	58.1%	53.8%
HACNN+DHA-NET [58]	91.3%	76.0%	81.3%	64.1%	-	-	-	-
IANet[43]	94.4%	83.1%	87.1%	73.4%	-	-	-	-
BDB[85]	94.2%	84.3%	86.8%	72.1%	72.8%	69.3%	73.6%	71.7%
AANet[4]	93.9%	83.4%	87.7%	74.3%	-	-	-	-
CAMA[61]	94.7%	84.5%	85.8%	72.9%	66.6%	64.2%	-	-
CBDB-Net	94.4%	85.0%	87.7%	74.3%	76.6%	72.8%	78.3%	75.9%
CBDB-Net+Re-ranking [79]	<b>95.6%</b>	<b>93.0%</b>	<b>91.2%</b>	<b>87.9%</b>	<b>83.9%</b>	<b>85.1%</b>	<b>86.5%</b>	<b>87.8%</b>

most existing methods on Market-1501 dataset. And then, we further introduce the Re-Ranking [79] into our CBDB-Net, i.e. CBDB-Net+Re-ranking. Here, the CBDB-Net+Re-ranking can achieve 95.6% Rank-1 and 93.0% mAP on the Market1501. On the DukeMTMC-reID dataset, our CBDB-Net obtains 87.7% Rank-1 and 74.3% mAP. The CBDB-Net+Re-ranking can achieve 91.2% Rank-1 and 87.9% mAP. The CUHK03 dataset is the most challenging dataset among the three generic person Re-ID datasets. Following the data setting in [84], [26], [85], [53], our CBDB-Net has clearly yielded good performance. On the CUHK03-Detected dataset, our CBDB-Net achieves 76.6% Rank-1 and 72.8% mAP; On the CUHK03-Labeled dataset, our CBDB-Net achieves 78.3% Rank-1 and 75.9% mAP. If we introduce the Re-ranking strategy into the CBDB-Net, the CBDB-Net+Re-ranking can further achieve 83.9% Rank-1 and 85.1% mAP on the CUHK03-Detected dataset and achieves 86.5% Rank-1 and 87.8% mAP on the CUHK03-Labeled dataset respectively.

In our CBDB-Net, the Consecutive DropBlock Module can produce multiple incomplete feature maps. We can regard the incomplete feature map as a kind of occluded or partial person feature. As shown in Figure 7, these incomplete feature tensors push the model to capture a robust person descriptor from the incomplete feature map for Re-ID in the training stage. So, we secondly try to evaluate the performance of our CBDB-Net in the occluded or partial person Re-ID task. We compared our CBDB-Net against the many approaches on Occluded DukeMTMC, Partial-REID, and Partial iLIDS, as shown in Table VI and Table VII respectively. On the Occluded DukeMTMC dataset, our CBDB-Net achieves the 50.9% Rank-1 and 38.9% mAP; On the Partial-REID dataset, our CBDB-Net achieves the 66.7% Rank-1 and 78.3% Rank-3; On the Partial iLIDS dataset, our CBDB-Net achieves the 68.4% Rank-1 and 81.5% Rank-3. From the Table VI

TABLE VI

THE COMPARISON WITH A SERIES OF OCCLUDED PERSON RE-ID METHODS IN OCCLUDED-DUKEMTMC DATASET. THE FIRST, SECOND AND THIRD HIGHEST SCORES ARE SHOWN IN RED, GREEN AND BLUE RESPECTIVELY.

Method	Occluded-DukeMTMC			
	Rank-1	Rank-5	Rank-10	mAP
LOMO+XQDA [33]	8.1%	17.0%	22.0%	5.0%
DIM [69]	21.5%	36.1%	42.8%	14.4%
Part Aligned [73]	28.8%	44.6%	51.0%	20.2%
Random Erasing [81]	40.5%	59.6%	66.8%	30.0%
HA-CNN [32]	34.4%	51.9%	59.4%	26.0%
Adver Occluded [24]	44.5%	-	-	32.2%
PCB [53]	42.6%	57.1%	62.9%	33.7%
Part Bilinear [52]	36.9%	-	-	-
FD-GAN [15]	40.8%	-	-	-
DSR [21]	40.8%	58.2%	65.2%	30.4%
SFR [22]	42.3%	60.3%	67.3%	32.0%
PGFA [38]	51.4%	68.6%	74.9%	37.3%
CBDB-Net	50.9%	66.0%	74.2%	38.9%

TABLE VII

THE COMPARISON WITH A SERIES OF OCCLUDED PERSON RE-ID METHODS IN PARTIAL-REID AND PARTIAL iLIDS DATASET. THE FIRST, SECOND AND THIRD HIGHEST SCORES ARE SHOWN IN RED, GREEN AND BLUE RESPECTIVELY.

Method	Partial-REID		Partial iLIDS	
	Rank-1	Rank-3	Rank-1	Rank-3
MTRC [34]	23.7%	27.3%	17.7%	26.1%
AMC+SWM [60]	37.3%	46.0%	21.0%	32.8%
DSR [21]	50.7%	70.0%	58.8%	67.2%
SFR [22]	56.9%	78.5%	63.9%	74.8%
PGFA [38]	68.0%	80.0%	69.1%	80.9%
CBDB-Net	66.7%	78.3%	68.4%	81.5%

to Table VII, on the occluded or partial person Re-ID task, our CBDB-Net achieves the competitive results on the three datasets. Compared with PGFA [38], the performance of our CBDB-Net is a little bit worse. However, the PGFA [38] needs

TABLE VIII  
THE COMPARISON ON RANK-1, RANK-10, AND RANK-20 WITH OTHER METHODS STANFORD ONLINE PRODUCTS DATASETS. THE FIRST, SECOND AND THIRD HIGHEST SCORES ARE SHOWN IN RED, GREEN AND BLUE RESPECTIVELY.

Method	In-Shop Clothes		
	Rank-1	Rank-10	Rank-20
FasionNet [37]	53.0%	73.0%	76.0%
HDC [70]	62.1%	84.9%	89.0%
DREML [67]	78.4%	93.7%	95.8%
HTL [14]	80.9%	94.3%	95.8%
A-BIER [39]	83.1%	95.1%	96.9%
ABE-8 [29]	87.3%	96.7%	97.9%
BDB [85]	89.1%	96.3%	97.6%
CBDB-Net	92.3 ± 0.3%	98.4 ± 0.2%	99.2 ± 0.2%



Fig. 10. The top-5 ranking list for the query person on CUHK03-Detected text set from the proposed CBDB-Net. The correct retrieval results are highlighted by green borders and the incorrect retrieval results by red borders.

the additional human model to extract the human landmark to help the model locate the key local feature. So, the structure of PGFA [38] is much more complex than that of our CBDB-Net. In contrast, our CBDB-Net needn't any auxiliary model, and is a kind of simple and efficient person Re-ID model.

In addition to the good performance in the two kind person Re-ID tasks, we believe that our CBDB-Net can be effective in other image retrieval tasks. We thirdly evaluate the performance of our CBDB-Net on the clothes retrieval task. As shown in Table VIII, our CBDB-Net also achieves a good performance on the In-shop clothes retrieval dataset.

Some sample query results are illustrated in Figure 10. We can see that, given a person image, CBDB-Net Network can effectively retrieve the same person images in the gallery set. However, there are retrieval negative results in Figure 10. In the third row of Figure 10, the query person was also mixed in other person images, which made the model confused

extract the suitable person feature. In the fourth row of Figure 10, the occlusion makes other features of the incorrectly retrieved person body very similar to query person image. Thus, it is necessary to further improve the CBDB-Net in the occlusion person Re-ID task in future works. Overall, our observations endorse the superiority of CBDB-Net by combing the ‘‘Consecutive Batch DropBlock Module’’ and ‘‘Elastic Loss’’. Compared with other state-of-the-art approaches, our model is simple and effective especially our testing mode. In our CBDB-Net, we only extract a 512 dimension global descriptor to conduct the person matching task and gain good performance.

## V. CONCLUSION

In this paper, we propose a novel person Re-ID model, Consecutive Batch DropBlock Network (CBDB-Net), to improve the ability of the person Re-ID model on capturing the robust and high-quality feature descriptor for the person matching. Specifically, firstly Consecutive Batch DropBlock Module is proposed to exploit multiple incomplete descriptors, which can effectively push the person Re-ID model to capture the robust feature descriptor. Secondly, the Elastic Loss is designed to adaptively mine and balance the hard sample pairs in the training process. Extensive experiments show that our CBDB-Net achieves the competitive performance on three generic person Re-ID datasets, three occlusion person Re-ID datasets, and the generic image retrieval task.

## REFERENCES

- [1] Tianlong Chen, Shaojin Ding, Jingyi Xie, Ye Yuan, Wuyang Chen, Yang Yang, Zhou Ren, and Zhangyang Wang. Abd-net: Attentive but diverse person re-identification. In *IEEE International Conference on Computer Vision*, 2019.
- [2] De Cheng, Yihong Gong, Sanping Zhou, Jinjun Wang, and Nanning Zheng. Person re-identification by multi-channel parts-based cnn with improved triplet loss function. In *IEEE Conference on Computer Vision and Pattern Recognition (CVPR)*, 2016.
- [3] De Cheng, Yihong Gong, Sanping Zhou, Jinjun Wang, and Nanning Zheng. Person re-identification by multi-channel parts-based cnn with improved triplet loss function. In *CVPR*, 2016.
- [4] Tay Chiat-Pin, Roy Sharmili, and Yap Kim-Hui. Aanet: Attribute attention network for person re-identifications. In *IEEE Conference on Computer Vision and Pattern Recognition*, 2019.
- [5] Yeong-Jun Cho and Kuk-Jin Yoon. Improving person reidentification via pose-aware multi-shot matching. In *IEEE Conference on Computer Vision and Pattern Recognition*, 2016.
- [6] Song Chunfeng, Huang Yan, Wang Liang, and Ouyang Wanli. Mask-guided contrastive attention model for person re-identification. In *IEEE Conference on Computer Vision and Pattern Recognition (CVPR)*, 2018.
- [7] Wanli Ouyang Chunfeng Song, Yan Huang and Liang Wang. Mask-guided contrastive attention model for person re-identification. In *IEEE Conference on Computer Vision and Pattern Recognition (CVPR)*, pages 1179–1188, 2018.
- [8] Jia Deng, Wei Dong, Richard Socher, Li-Jia Li, Kai Li, and Li Fei-Fei. Imagenet: A large-scale hierarchical image database. In *CVPR*, 2009.
- [9] Weijian Deng, Zheng Liang, Guoliang Kang, Yang Yi, and Jianbin Jiao. Image-image domain adaptation with preserved self-similarity and domain-dissimilarity for person re-identification. In *IEEE Conference on Computer Vision and Pattern Recognition (CVPR)*, pages 994–1003, 2018.
- [10] Terrance DeVries and Graham W Taylor. Improved regularization of convolutional neural networks with cutout. In *arXiv:1708.04552*, 2017.
- [11] Fartash Faghri, David J. Fleet, Jamie Ryan Kiros, and Sanja Fidler. Vse++: Improved visual-semantic embeddings. In *BMVC*, 2018.
- [12] Liu Fangyi and Zhang Lei. View confusion feature learning for person re-identification. In *IEEE International Conference on Computer Vision*, 2019.

- [13] Zhanxiang Feng, Jianhuang Lai, and Xiaohua Xie. Learning view-specific deep networks for person re-identification. *IEEE Transactions on Image Processing*, 27(7):3472 – 3483, 2018.
- [14] Weifeng Ge, Weilin Huang, Dengke Dong, and Matthew RScott. Deep metric learning with hierarchical triplet loss. In *ECCV*, 2018.
- [15] Yixiao Ge, Zhuowan Li, Haiyu Zhao, Guojun Yin, Shuai Yi, and Xiaogang Wang. Fd-gan: Pose-guided feature distilling gan for robust person re-identification. In *NIPS*, 2018.
- [16] Mengyue Geng, Yaowei Wang, Tao Xiang, and Yonghong Tian. Deep transfer learning for person re-identification. 2016.
- [17] Golnaz Ghiasi, Tsung-Yi Lin, and Quoc V Le. Dropblock: A regularization method for convolutional networks. In *arXiv:1810.12890*, 2018.
- [18] Priya Goyal, Piotr Dollár, Ross Girshick, Pieter Noordhuis, Lukasz Wesolowski, Aapo Kyrola, Andrew Tulloch, Yangqing Jia, and Kaiming He. Accurate, large minibatch sgd: Training imagenet in 1 hour. In *arXiv:1706.02677*, 2017.
- [19] Jianyuan Guo, Yuhui Yuan, Lang Huang, Chao Zhang, Jin-Ge Yao, and Kai Han. Beyond human parts: Dual part-aligned representations for person re-identification. In *ICCV*, 2019.
- [20] Kaiming He, Xiangyu Zhang, Shaoqing Ren, and Jian Sun. Deep residual learning for image recognition. In *CVPR*, 2016.
- [21] Lingxiao He, Jian Liang, Haiqing Li, and Zhenan Sun. Deep spatial feature reconstruction for partial person reidentification: Alignment-free approach. In *CVPR*, 2018.
- [22] Lingxiao He, Zhenan Sun, Yuhao Zhu, and Yunbo Wang. Recognizing partial biometric patterns. In *arXiv preprint arXiv:1810.07399*, 2018.
- [23] Alexander Hermans, Lucas Beyer, and Bastian Leibe. In defense of the triplet loss for person re-identification. In *arXiv:1703.07737*, 2017.
- [24] Houjing Huang, Dangwei Li, Zhang Zhang, Xiaotang Chen, and Kaiqi Huang. Adversarially occluded samples for person re-identification. In *CVPR*, 2018.
- [25] Tang Jinhui, Shu Xiangbo, Yan Rui, and Zhang Liyan. Coherence constrained graph lstm for group activity recognition. In *IEEE Transactions on Pattern Analysis and Machine Intelligence (TPAMI)*, 2019.
- [26] Zhou Kaiyang, Yang Yongxin, Cavallaro Andrea, and Xiang Tao. Omniscale feature learning for person re-identification. In *IEEE International Conference on Computer Vision*, 2019.
- [27] Mahdi M. Kalayeh, Emrah Basaran, Muhittin Gokmen, Mustafa E. Kamasak, and Mubarak Shah. Human semantic parsing for person re-identification. In *IEEE Conference on Computer Vision and Pattern Recognition (CVPR)*, 2018.
- [28] Mahdi M Kalayeh, Emrah Basaran, Muhittin Gokmen, Mustafa E Kamasak, and Mubarak Shah. Human semantic parsing for person re-identification. In *IEEE Conference on Computer Vision and Pattern Recognition (CVPR)*, 2018.
- [29] Wonsik Kim, Bhavya Goyal, Kunal Chawla, Jungmin Lee, , and Keunjoo Kwon. Attention-based ensemble for deep metric learning. In *ECCV*, 2018.
- [30] Diederik P Kingma and Jimmy Ba. Adam: A method for stochastic optimization. In *ICLR*, 2015.
- [31] Wei Li, Rui Zhao, Tong Xiao, and Xiaogang Wang. Deepreid: Deep filter pairing neural network for person reidentification. In *IEEE Conference on Computer Vision and Pattern Recognition*, 2014.
- [32] Wei Li, Xiatian Zhu, and Shaogang Gong. Harmonious attention network for person re-identification. In *IEEE Conference on Computer Vision and Pattern Recognition (CVPR)*, pages 2285–2294, 2018.
- [33] Shengcai Liao, Yang Hu, Xiangyu Zhu, and Stan Z. Li. Person re-identification by local maximal occurrence representation and metric learning. In *IEEE Conference on Computer Vision and Pattern Recognition (CVPR)*, pages 2197–2206, 2015.
- [34] Shengcai Liao, Anil K Jain, and Stan Z Li. Partial face recognition: Alignment-free approach. In *TPAMI*, 2013.
- [35] Tsung Yi Lin, Priya Goyal, Ross Girshick, Kaiming He, and Piotr Dollár. Focal loss for dense object detection. *IEEE Transactions on Pattern Analysis and Machine Intelligence*, PP(99):2999–3007, 2017.
- [36] Yutian Lin, Zheng Liang, Zhedong Zheng, Wu Yu, and Yang Yi. Improving person re-identification by attribute and identity learning. 2017.
- [37] Ziwei Liu, Ping Luo, Shi Qiu, Xiaogang Wang, and Xiaoou Tang. Deepfashion: Powering robust clothes recognition and retrieval with rich annotations. In *CVPR*, 2016.
- [38] Jiayu Miao, Yu Wu, Ping Liu, Yuhang Ding, and Yi Yang. Pose-guided feature alignment for occluded person re-identification. In *IEEE International Conference on Computer Vision*, 2019.
- [39] Michael Opitz, Georg Waltner, Horst Possegger, and Horst Bischof. Deep metric learning with bier: Boosting independent embeddings robustly. In *IEEE transactions on pattern analysis and machine intelligence*, 2018.
- [40] Xuelin Qian, Yanwei Fu, Tao Xiang, Wenxuan Wang, Jie Qiu, Yang Wu, Yu-Gang Jiang, and Xiangyang Xue. Pose normalized image generation for person re-identification. In *European Conference on Computer Vision*, 2018.
- [41] Ergys Ristani, Francesco Solera, Roger Zou, Rita Cucchiara, and Carlo Tomasi. Performance measures and a data set for multi-target, multi-camera tracking. In *European Conference on Computer Vision (ECCV)*, 2016.
- [42] Yan Rui, Xie Lingxi, Tang Jinhui, Shu Xiangbo, and Tian Qi. Hgcin: Hierarchical graph-based cross inference network for group activity recognition. In *IEEE Transactions on Pattern Analysis and Machine Intelligence (TPAMI)*, 2019.
- [43] Hou Ruibing, Ma Bingpeng, Chang Hong, Gu Xinqian, Shan Shiguang, and Chen Xilin. Interaction-and-aggregation network for person re-identification. In *IEEE Conference on Computer Vision and Pattern Recognition*, 2019.
- [44] Zhou Sanping, Wang Fei, Huang Zeyi, and Wang Jinjun. Discriminative feature learning with consistent attention regularization for person re-identification. In *IEEE International Conference on Computer Vision*, 2019.
- [45] Zhou Sanping, Wang Jinjun, Meng Deyu, Liang Yudong, Gong Yihong, and Zheng Nanning. Discriminative feature learning with foreground attention for person re-identification. *IEEE Transactions on Image Processing*, 28(9):4671 – 4684, 2019.
- [46] M. Saquib Sarfraz, Arne Schumann, Andreas Eberle, and Rainer Stiefelhagen. A pose-sensitive embedding for person re-identification with expanded cross neighborhood reranking. In *CVPR*, 2018.
- [47] Florian Schroff, Dmitry Kalenichenko, and James Philbin. Facenet: A unified embedding for face recognition and clustering. In *CVPR*, 2015.
- [48] Chen Shen, Guo Jun Qi, Rongxin Jiang, Zhongming Jin, Hongwei Yong, Yaowu Chen, and Xian Sheng Hua. Sharp attention network via adaptive sampling for person re-identification. In *IEEE Transactions on Circuits and Systems for Video Technology*, 2018.
- [49] Guangrun Wang Shengyong Ding an Liang Lin and Hongyang Chao. Deep feature learning with relative distance comparison for person re-identification. *Pattern Recognition*, 48(10):2993–3003, 2015.
- [50] Nitish Srivastava, Geoffrey Hinton, Alex Krizhevsky, Ilya Sutskever, and Ruslan Salakhutdinov. Dropout: a simple way to prevent neural networks from overfitting. In *JMLR*, 2014.
- [51] Chi Su, Jianing Li, Shiliang Zhang, Junliang Xing, Wen Gao, and Qi Tian. Pose-driven deep convolutional model for person re-identification. In *IEEE International Conference on Computer Vision*, 2017.
- [52] Yumin Suh, Jingdong Wang, Siyu Tang, Tao Mei, and Kyoung Mu Lee. Part-aligned bilinear representations for person re-identification. In *ECCV*, 2018.
- [53] Yifan Sun, Liang Zheng, Yi Yang, Qi Tian, and Shengjin Wang. Beyond part models: Person retrieval with refined part pooling (and a strong convolutional baseline). In *Proceedings of the European Conference on Computer Vision (ECCV)*, 2018.
- [54] Jonathan Tompson, Ross Goroshin, Arjun Jain, Yann LeCun, and Christoph Bregler. Efficient object localization using convolutional networks. In *CVPR*, 2015.
- [55] Rahul Rama Varior, Mrinal Haloi, and Wang Gang. Gated siamese convolutional neural network architecture for human re-identification. In *European Conference on Computer Vision (ECCV)*, 2016.
- [56] Cheng Wang, Qian Zhang, Chang Huang, Wenyu Liu, and Xinggang Wang. Mancs: A multi-task attentional network with curriculum sampling for person re-identification. In *Proceedings of the European Conference on Computer Vision (ECCV)*, 2018.
- [57] Guan'an Wang, Shuo Yang, Huanyu Liu, Zhicheng Wang, Yang Yang, Shuliang Wang, Gang Yu, Erjin Zhou, and Jian Sun. High-order information matters: Learning relation and topology for occluded person re-identification. In *CVPR*, 2020.
- [58] Zheng Wang, Junjun Jiang, Yang Wu, Mang Ye, Xiang Bai, and Shinichi Satoh. Learning sparse and identity-preserved hidden attributes for person re-identification. *IEEE Transactions on Image Processing*, 29:2013 – 2025, 2020.
- [59] Longhui Wei, Shiliang Zhang, Hantao Yao, Wen Gao, and Qi Tian. Glad: Global-local-alignment descriptor for pedestrian retrieval. In *ACM MM*, 2017.
- [60] Tao Xiang Shengcai Liao Jianhuang Lai Wei-Shi Zheng, Xiang Li and Shaogang Gong. Partial person reidentification. In *ICCV*, 2015.
- [61] Yang Wenjie, Huang Houjing, Zhang Zhang, Chen Xiaotang, Huang Kaiqi, and Zhang. Shu. Towards rich feature discovery with class activation maps augmentation for person re-identification. In *IEEE Conference on Computer Vision and Pattern Recognition*, 2019.
- [62] Bryan (Ning) Xia, Yuan Gong, Yizhe Zhang, and Christian Poellabauer. Second-order non-local attention networks for person re-identification. In *IEEE International Conference on Computer Vision*, 2019.
- [63] Shu Xiangbo, Tang Jinhui, Qi Guojun, Liu Wei, and Yang Jian. Hierarchical long short-term concurrent memory for human interaction

- recognition. In *IEEE Transactions on Pattern Analysis and Machine Intelligence (TPAMI)*, 2019.
- [64] Shu Xiangbo, Zhang Liyan, Qi Guo-Jun, Liu Wei, and Tang Jinhui. Spatiotemporal co-attention recurrent neural networks for human-skeleton motion prediction. In *IEEE Transactions on Pattern Analysis and Machine Intelligence (TPAMI)*, 2019.
- [65] Chang Xiaobin, M Hospedales Timothy, and Xiang Tao. Multi-level factorisation net for person re-identification. In *IEEE Conference on Computer Vision and Pattern Recognition*, 2018.
- [66] Jing Xu, Rui Zhao, Feng Zhu, Huaming Wang, and Wanli Ouyang. Attention-aware compositional network for person re-identification. In *IEEE Conference on Computer Vision and Pattern Recognition*, 2018.
- [67] Hong Xuan, Richard Souvenir, and Robert Pless. Deep randomized ensembles for metric learning. In *ECCV*, 2018.
- [68] Hantao Yao, Shiliang Zhang, Yongdong Zhang, Jintao Li, and Qi Tian. Deep representation learning with part loss for person re-identification. In *arXiv:1707.00798*, 2017.
- [69] Qian Yu, Xiaobin Chang, Yi-Zhe Song, Tao Xiang, and Timothy M Hospedales. The devil is in the middle: Exploiting mid-level representations for cross-domain instance matching. In *arXiv:1711.08106*, 2017.
- [70] Yuhui Yuan, Kuiyuan Yang, and Chao Zhang. Hard-aware deeply cascaded embedding. In *ICCV*, 2017.
- [71] Xiang T. Gong S. Zhang, L. Learning a discriminative null space for person re-identification. In *IEEE Conference on Computer Vision and Pattern Recognition (CVPR)*, pages 1335–1344, 2016.
- [72] Haiyu Zhao, Maoqing Tian, Shuyang Sun, Jing Shao, Junjie Yan, Shuai Yi, Xiaogang Wang, and Xiaoou Tang. Spindle net: Person re-identification with human body region guided feature decomposition and fusion. In *CVPR*, 2017.
- [73] Liming Zhao, Xi Li, Yueting Zhuang, and Jingdong Wang. Deeply-learned part-aligned representations for person re-identification. In *IEEE International Conference on Computer Vision (ICCV)*, 2017.
- [74] Zheng Zhedong, Zheng Liang, and Yang Yi. Pedestrian alignment network for large-scale person re-identification. *IEEE Transactions on Circuits and Systems for Video Technology*, 29(10):3037–3045, 2019.
- [75] Yi Yang Zhedong Zheng, Liang Zheng. Unlabeled samples generated by gan improve the person re-identification baseline in vitro. In *International Conference on Computer Vision (ICCV)*, 2017.
- [76] Liang Zheng, Liyue Shen, Lu Tian, Shengjin Wang, Jingdong Wang, and Qi Tian. Scalable person re-identification: A benchmark. In *IEEE International Conference on Computer Vision (ICCV)*, pages 1116–1124, 2015.
- [77] Liang Zheng, Yi Yang, and Alexander G. Hauptmann. Person re-identification: Past, present and future. 2016.
- [78] Zhedong Zheng, Liang Zheng, and Yi Yang. Pedestrian alignment network for large-scale person re-identification. In *IEEE Transactions on Circuits and Systems for Video Technology*, 2017.
- [79] Zhun Zhong, Liang Zheng, Donglin Cao, and Shaozi Li. Re-ranking person re-identification with k-reciprocal encoding. In *IEEE Conference on Computer Vision and Pattern Recognition (CVPR)*, 2017.
- [80] Zhun Zhong, Liang Zheng, Guoliang Kang, Shaozi Li, and Yi Yang. Random erasing data augmentation. In *arXiv:1708.04896*, 2017.
- [81] Zhun Zhong, Liang Zheng, Guoliang Kang, Shaozi Li, and Yi Yang. Random erasing data augmentation. In *arXiv:1708.04896*, 2017.
- [82] Zhun Zhong, Liang Zheng, Zhedong Zheng, Shaozi Li, and Yi Yang. CamStyle: A novel data augmentation method for person re-identification. *IEEE Transactions on Image Processing*, 28(3):1176–1190, mar 2019.
- [83] Jianqing Zhu, Huanqiang Zeng, Shengcai Liao, Zhen Lei, Canhui Cai, and Lixin Zheng. Deep hybrid similarity learning for person re-identification. In *IEEE Transactions on Circuits and Systems for Video Technology*, 2017.
- [84] Zhong Zhun, Zheng Liang, Kang Guoliang, Li Shaozi, and Yang Yi. Random erasing data augmentation. In *The National Conference on Artificial Intelligence*, 2020.
- [85] Dai Zuo Zhuo, Chen Mingqiang, Gu Xiaodong, Zhu Siyu, and Tan Ping. Batch dropout network for person re-identification and beyond. In *IEEE International Conference on Computer Vision*, 2019.